Hybrid Coupler Utilizing Substrate Integrated Waveguide (SIW) Technology for Ka-Band Applications

Osamah Ali Mohsin, and Alyani bt. Ismail

***Abstract*—This paper introduces a hybrid coupler based on SIW technology at 26 GHz and 28 GHz. High losses from the components due to the low wavelength are expected at Ka-band, primarily when planar technology is implemented. Hence, SIW structures are introduced to overcome these losses. A designed coupler based on the direct coupling vias method is proposed in this work. Two rows of vias are implemented with a coupling aperture between them, with cutting in the SIW narrow wall of the SIW. Using this technique benefits in controlling the coupling and the phase differences of the coupler outputs. The designed Coupler is simulated using CST software and metal printed to validate the Coupler's performance. The measured reflection and isolation coefficients are less than -20 dB at 26 GHz and 28 GHz, with transmission coefficients ranging between -2.9 dB and -3.6 dB. The phase differences of -87.2° are observed at the outputs. Overall, the printed SIW coupler has excellent potential for Ka-band applications.**

***Index Terms*—Direct coupling, Hybrid Coupler, SIW, Ka bands.**

I. Introduction

Beamforming networks play a crucial role in fifth-generation (5G) wireless communication systems, as they are expected to provide high-gain directive beams and wideband data rates. Additionally, these networks aim to offer low-loss and low-profile, state-of-the-art 5G devices. However, achieving a reliable beamforming network relies heavily on the accurate design of the coupler circuit, which must deliver equal outputs and the correct phase difference at those outputs. Couplers are significant components within beamforming networks, as they control both the phase difference and the magnitude of the outputs [1], [2], [5], [6], [11], [12].

Typically, a hybrid coupler configuration consists of two inputs and two outputs, with a 3 dB power split and a 90° phase difference. When the input ports are activated, two uniform amplitudes with different phases are generated at the outputs. Various couplers have been proposed for 5G beamforming networks, such as microstrip couplers, substrate integrated waveguide (SIW) couplers, and other types of SIW couplers. However, microstrip couplers often suffer from high loss in transmission lines and fabrication tolerance issues at higher frequencies. Moreover, planar substrate couplers can lead to unwanted crosstalk between output ports due to the small distance between the coupled lines. This results in increased insertion loss and larger phase errors [4], [8], [10], [20], [19], [22].

To address these challenges, a waveguide-based structure is proposed as a potential solution to mitigate these losses and phase error issues. Waveguide structures help reduce crosstalk among the outputs and enhance SIW aperture coupling. Additionally, an SIW coupler utilizing cavity resonators has been introduced as a promising approach for high-frequency applications. However, this method has demonstrated a narrow bandwidth and significant size limitations.

As a solution, direct coupling in waveguide-based structures simplifies phase control, resulting in fewer phase difference errors at the outputs. Therefore, this paper proposes a rectangular SIW direct coupling design, which aims to provide equal power and phase differences [9], [13], [14], [16], [18], [21].

The key contributions of this work are as follows:

- A new Ka-band hybrid coupler is suggested, which is made of substrate integrated waveguide (SIW) technology, with frequencies of 26 GHz and 28 GHz, which is particular to low-loss beamforming networks in 5G millimeter-wave systems.
- It presents a direct coupling method with dual rows of vias having a modified narrow-wall aperture that allows a controlled coupling level and phase difference with a direct coupling technique that has much lower transmission loss and unwanted crosstalk as compared to planar and conventional SIW couplers.
- A systematic parametric study of the width of the narrow walls and the size of the coupling aperture is undertaken, which gives design insights on the design of impedance matching, isolation enhancement, as well as precise 3-dB power division in the Ka-band frequencies.
- It provides an ultra-wide impedance bandwidth of over 7 GHz, significantly larger than the Ka-band SIW couplers reported previously, and thus the design can be applied in multi-band 5G beamforming systems.
- The designed SIW coupler is realized and experimentally confirmed with reported insertion losses of less than -2.9

Manuscript received January 28, 2026; revised February 15, 2026. Date of publication August 26, 2026. Date of current version August 26, 2026. The associate editor prof. Miroslav Joler has been coordinating the review of this manuscript and approved it for publication.

O. A. Mohsin is with the University of Technology, Baghdad, Iraq (e-mail: usama.a.mohsen@uotechnology.edu.iq).

A. bt. Ismail is with the Universiti Putra Malaysia, Malaysia (e-mail: alyani@upm.edu.my).

Digital Object Identifier (DOI): 10.24138/jcomss-2025-0294

dB to less than -3.6 dB, isolation less than -20 dB, and a constant quadrature phase difference of 87.2° indicating very well the outcomes of simulation work.

- A detailed comparison of it with the state-of-the-art Ka-band hybrid couplers is given, which proves that the proposed design has better bandwidth and lower phase error, and competitive loss characteristics.

The paper presents a waveguide-based coupler designed by introducing an aperture between two rectangular waveguides using a modified narrow wall method, focusing on frequencies of 26 GHz and 28 GHz. The designed structure is simulated using CST software and validated through performance measurements. The paper is organized as follows: Section II discusses the design methodology of the SIW coupler, Section III presents the results and discussion of the printed coupler, and Section IV concludes the paper.

Even though the coupler was designed to work mostly at 26 GHz and 28 GHz, the distributed aperture coupling mechanism of SIW inherently results in a broader frequency spectrum of impedance. This broadband response is better than dealing with fabrication variations and frequency drift, and also, the multi-channel and wideband beamforming can be operated in 5G systems in practice.

II. Design of Hybrid Coupler based on Direct Coupling SIW Architecture

The waveguide-based structure used in this work is chosen with inner dimensions of WR-34 [14]. The cut-off frequency (f_c) and guided wavelength (λ_g) of the SIW can be calculated using the following:

$$f_{c_{mn}} = \frac{c}{2\sqrt{\varepsilon_r}} \sqrt{\left(\frac{m}{a}\right)^2 + \left(\frac{n}{b}\right)^2} \quad (1)$$

$$\lambda_g = \frac{\lambda_0}{\sqrt{1-\left(\frac{f_c}{f}\right)^2}} \quad (2)$$

The inner dimensions are a and b, the number of TE modes is m and n, the speed of light is c, and λ_0 is the wavelength in space. In this case, TE_{10} mode is operated in the SIW, which denotes a half-wavelength of field variations.

Figure 1 illustrates the proposed hybrid coupler constructed from two SIW rectangular waveguides utilizing an aperture SIW coupling technique along with a modified SIW narrow wall. Two long SIW rectangular quarter-wavelength (λ/4) transmission lines are integrated, featuring a direct coupling aperture positioned between them. The outputs of the coupler are linked through a narrow wall direct coupling with an electrical length of a quarter wavelength (λ/4). This direct coupling approach is employed to ensure that power is evenly divided at the outputs of the coupler [21], [16], [20], [19].

To analyze the designed Coupler's response, a parametric study is performed using CST software with the following parameters: the width of the narrow wall (W) and the width of the aperture (W2). Figure 2 shows the simulation results of the reflection, isolation, and transmission coefficients varying with cutting in the narrow wall width and the aperture coupling width [3], [10], [12], [13].

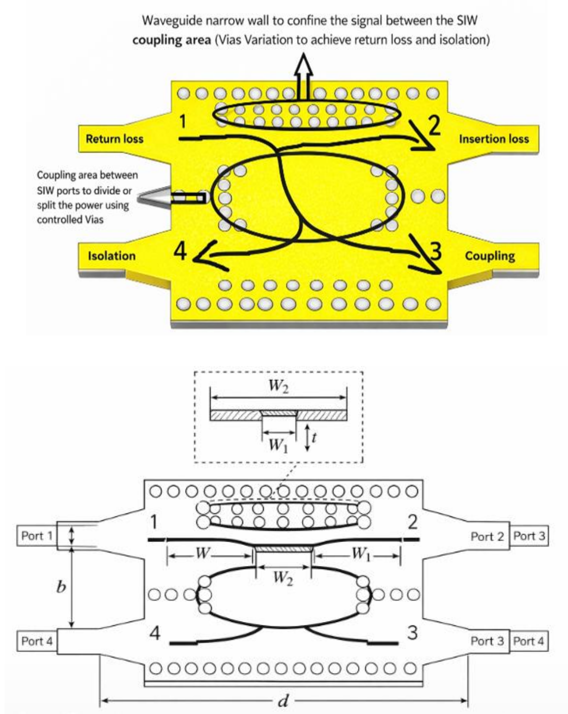

Fig. 1. Structure of the SIW coupler using vias direct coupling aperture.

In Figure 2(a), it can be observed that the frequency shifts to a lower band as the width of the narrow wall increases. Additionally, the width of the aperture influences the output, producing unequal power distribution away from a -3 dB coupling ratio. As the width of cutting W1 increases, both impedance matching and the reflection coefficient are affected. Consequently, the final dimensions of the proposed coupler are derived from the parametric study and summarized in Table I.

Figure 3 illustrates the final design of the coupler along with the simulation results. The designed coupler, shown in Figure 3(a), features E-bend arms that are necessary for fabrication. These arms are added due to the minimal distance between ports, which complicates measurements using adaptors without them. The reflection coefficient S11 is -35 dB, indicating good return loss and a bandwidth exceeding 10 GHz. This bandwidth encompasses both the 26 GHz and 28 GHz bands. Power is evenly distributed between ports 2 and 3, with S21 = -2.97 dB and S31 = -3.04 dB, indicating a successful power split of 3 dB between the output ports. The isolation is less than -20 dB, and there is a 90° phase difference between the output ports, as shown in Figures 3(b), 3(c), and 3(d) [18], [9], [8].

To enhance independence of findings, the dimensional parameters used in Table I are clearly labelled in the design of Figure 1 to clearly show the correlation between the coupling aperture, narrow wall width, and SIW waveguide architecture.

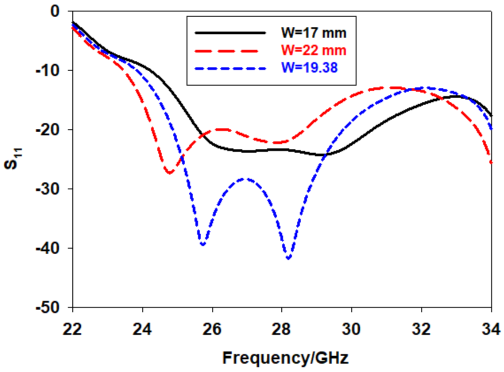

(a)

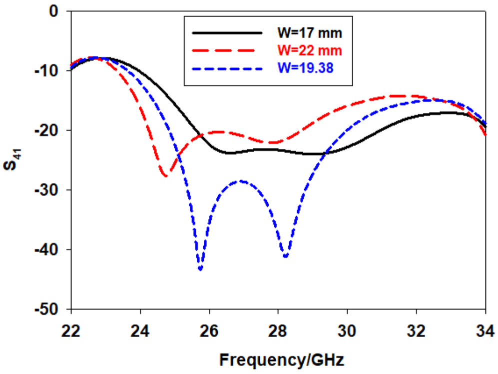

(b)

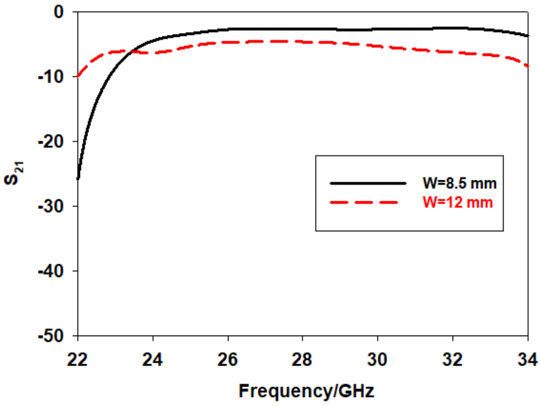

(c)

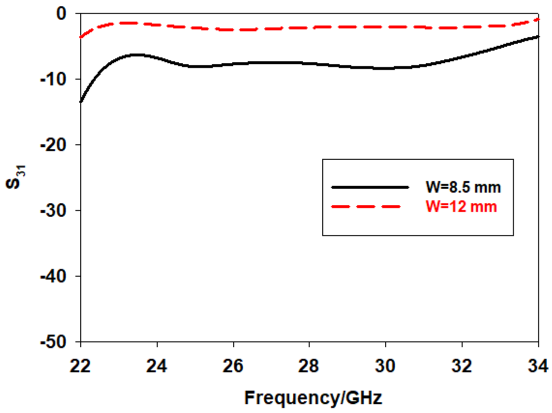

(d)

Fig. 2. Simulated response. (a) Reflection, (b) isolation, (c) port 2, (d) port 3.

TABLE I
DIMENSION OF THE PROPOSED COUPLER

Dim	Definition	Value (mm)
$a \times b$	Inner dim of waveguide	8.636 × 4.318
d	SIW length	50
W	Width of narrow wall	19.38
$W1$	Inner narrow wall	6.46
$W2$	Coupling area	10.812
t	Thickness of coupling	2.72

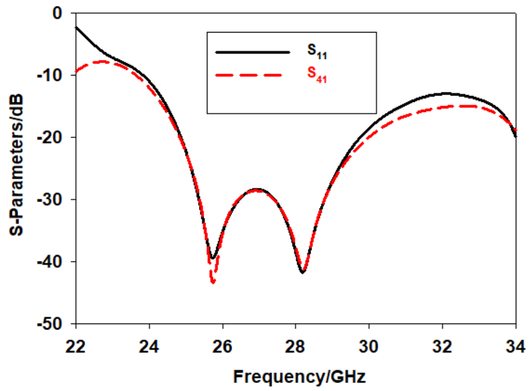

(a)

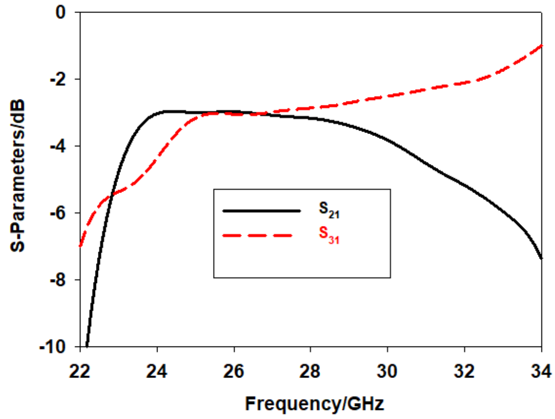

(b)

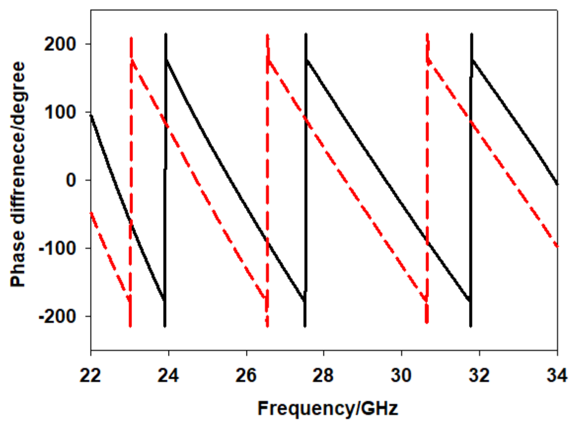

(c)

Fig. 3. The simulated results of the proposed Coupler. (a) Reflection and isolation. (b) Coupling at outputs. (c) Phase difference at outputs.

It is necessary to note that the introduction of the E-bend arms was done only to allow the practicality of measurement and access to the connector, as there were very short interfaces between ports at the Ka-band frequencies. In integrated implementations, these bends are not necessary, and the coupler may simply be connected to neighboring SIW routing or multilayer transitions. Thus, the small size of the port is not a constraint to realistic application and is advantageous to high-density millimeter-wave beamforming synthesis.

III. Experimental Results and Measurements Setup

Figure 4 shows the printed Coupler and the S-parameters measurement process. Port 1 was stimulated during measurement, Ports 2 and 3 were measured as output ports, and Port 4 (isolation port) was terminated with a matched 50 Ω load. The Keysight FieldFox N9925A was used in two-port measurement mode. A full two-port SOLT calibration was performed at the connector reference plane. Phase reference alignment was conducted prior to measurement. No additional de-embedding was applied beyond connector-plane calibration. 2.92 mm (K-type) connectors rated up to 40 GHz were used. Precision 50 Ω matched loads with return loss > 20 dB were employed. Estimated measurement uncertainty was approximately ±0.3 dB in magnitude and ±1° in phase at 28 GHz, based on VNA specification and calibration limits. The Coupler's S-parameters and phase difference performance are compared with simulated results in Figure 5 [8], [13].

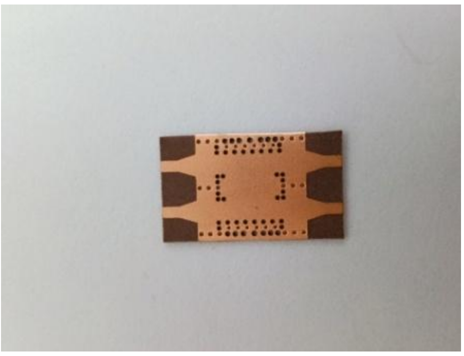

Fig. 4. The fabrication and Measurement process of the SIW printed Coupler.

The measured return loss (S_{11}) and isolation (S_{41}) results presented in Figure 5 (a) and Figure 5 (b) indicate that the proposed coupler achieves a wide bandwidth of 7 GHz, specifically within the range of 23 GHz to 30 GHz. At the target frequencies of 26 GHz and 28 GHz, the measured insertion loss (S_{21}) and coupling loss (S_{31}) demonstrate an evenly split power distribution across ports 2 and 3, measuring -3.6 dB and -2.92 dB, respectively, as illustrated in Figure 5 (c). The observed phase difference between port 2 and port 3 is 87.2°, in contrast to the simulated value of 90°, resulting in a phase error of 2.8° within the desired 90° phase difference.

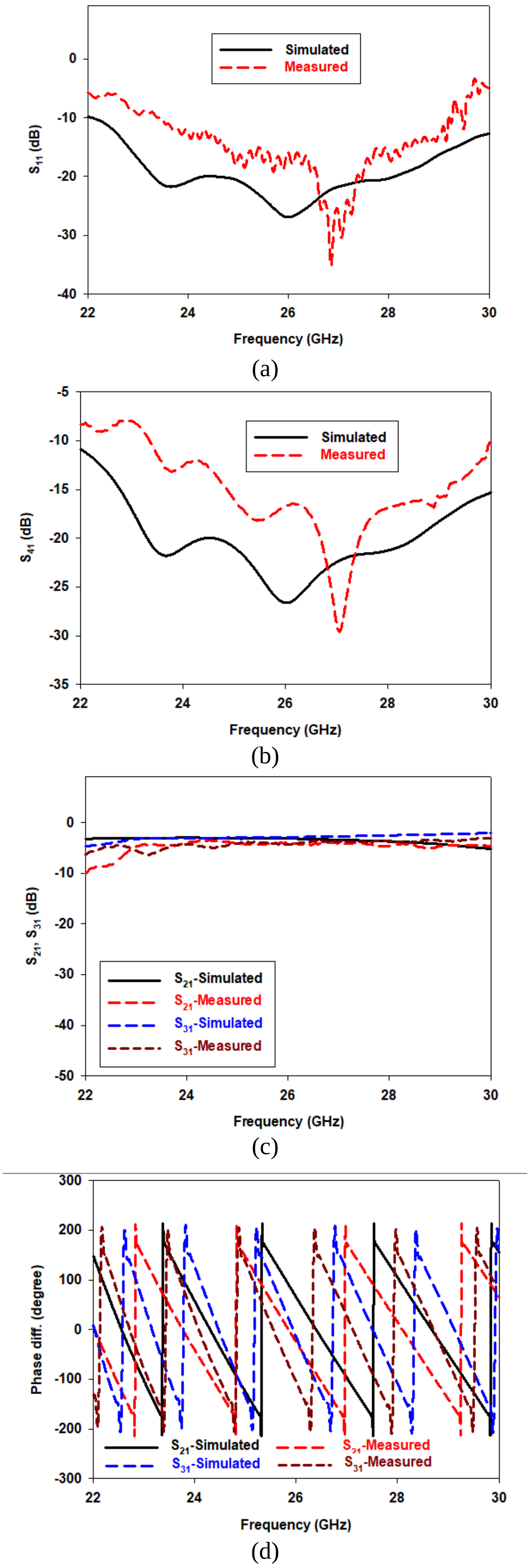

Fig. 5. Measured and Simulated comparison of the printed Coupler. (a) Reflection coefficient, (b) Isolation, (c) Transmission coefficients, (d) Phase difference.

The measured return loss (S_{11}) and isolation (S_{41}) results presented in Figure 5 (a) and Figure 5 (b) indicate that the proposed coupler achieves a wide bandwidth of 7 GHz, specifically within the range of 23 GHz to 30 GHz. At the target frequencies of 26 GHz and 28 GHz, the measured insertion loss (S_{21}) and coupling loss (S_{31}) demonstrate an evenly split power distribution across ports 2 and 3, measuring -3.6 dB and -2.92 dB, respectively, as illustrated in Figure 5 (c). The observed phase difference between port 2 and port 3 is 87.2°, in contrast to the simulated value of 90°, resulting in a phase error of 2.8° within the desired 90° phase difference. The observed differences (approximately 7–8 dB in return loss and isolation) are primarily attributed to fabrication tolerances via diameter and aperture width, dielectric constant variation of the substrate, and connector-to-SIW transition mismatch. At Ka-band (26–28 GHz), where the wavelength is approximately 11 mm, dimensional deviations as small as ±0.05 mm significantly affect impedance matching and coupling balance. Additionally, conductor surface roughness and finite metallization thickness introduce extra loss not fully modeled in the simulation. These practical effects explain the slight degradation in S11 and S41 while still maintaining acceptable performance for beamforming applications.

The primary design objective was reliable operation at the 26 GHz and 28 GHz 5G millimeter-wave bands. However, the direct-coupling SIW aperture structure inherently provides a broader impedance bandwidth (~7 GHz from 23–30 GHz). This wideband behavior is not accidental but results from the distributed coupling mechanism and reduced resonant dependency compared to cavity-based couplers.

A comparative analysis of the printed coupler alongside previously published works is summarized in Table II. Thus, the proposed coupler exhibits low-loss characteristics and ultra-wideband performance, aligning well with the primary requirements for 5G systems and applications in the millimeter wave spectrum [17], [12], [10], [21], [20].

TABLE II
COMPARISON BETWEEN SIMULATED AND MEASUREMENT RESULTS AND OTHER RELATED WORKS AT KA-BAND.

Parameters/Coupler	SIW Coupler at 26 GHz		SIW Coupler at 28 GHz	
	Simulated	Measured	Simulated	Measured
Return loss (S_{11})	-27 dB	-19 dB	-22 dB	-18 dB
Isolation (S_{41})	-26 dB	-18 dB	-23 dB	-17 dB
Direct (S_{21})	-2.99 dB	-2.77 dB	-3.05 dB	-2.90 dB
Coupling (S_{31})	-3.02 dB	-2.85 dB	-3.12 dB	-3.62 dB
FBW (%)	30	28	30	27
Phase diff. (degree)	90	88.2	89.5	87.2

Besides bandwidth and phase error, the proposed SIW coupler has other benefits of being easy to fabricate and more cost-effective. The architecture is based on standard SIW technology and metal printing, and can be used together with current Printed Circuit Board (PCB) manufacturing and waveguide manufacturing processes. The proposed design is simpler to fabricate in comparison to conventional waveguide couplers.

Moreover, SIW structures are excellent in terms of mechanical stability and environmental robustness, hence can be used in various environmental conditions.

TABLE III
COMPARISON BETWEEN THIS WORK AND OTHER RELATED WORKS AT KA-BAND

Ref / Year	Technology	BW (GHz)	Output Power (dB)	Phase Error (°)	Insertion Loss (dB)	Structure Complexity	Fabrication Method
[13] / 2022	Waveguide	3	-3.35	4.8°	-7 dB	Moderate (Metal 3D print)	Additive manufacturing
[12] / 2025	Ridge Gap WG	1.5	-4.5	15°	-6 dB	High (3D integration)	Advanced fabrication
[14] / 2024	Transformer-based	3.5	-5	9°	-9 dB	High (CMOS integration)	IC fabrication
[15] / 2024	3D Printed	0.25	-4.2	3.7°	-10 dB	Complex	Additive + DGS
This Work	SIW Direct Coupling	7	-3.62 / -2.9	2.8°	-5 to -7 dB	Low (Planar SIW)	Standard PCB + SIW vias

IV. Conclusion

This paper presents a low-loss hybrid coupler designed for Ka-band applications, utilizing waveguide-based direct coupling apertures. The coupler features two rectangular waveguides and a modified narrow wall. Both the measured and simulated results show good agreement. The measurements indicate an impedance bandwidth exceeding 7 GHz, with a minimum reflection coefficient of -18 dB at 26 GHz. A 3-dB coupling ratio was achieved at the output ports, along with a precise phase difference of 87.2° over the bandwidth. This coupler holds significant potential for use in beamforming networks for Ka-band applications.

References

[1] H. O. Otieno, B. Malila and J. Mwangama, "Deployment and Management of Intelligent End-to-End Network Slicing in 5G and Beyond 5G Networks: A Systematic Review," in *IEEE Access*, vol. 12, pp. 190411-190433, 2024.

[2] S. Montoya-Villada, J. Morales-Guerra, D. Catano-Ochoa, J. Zapata-Londono, J. Botero-Valencia, and E. Reyes-Vera, "Design and Implementation of a 2.4-GHz Fully Integrated Butler Matrix for Smart Antenna System," *International Journal on Communications Antenna and Propagation (IRECAP)*, vol. 13, no. 1, pp. 1–1, Feb. 2023.

[3] I. Peshkov, V. Zhigulin, and N. Fortunova, "Simulation Study of the Direction-of-Arrival Estimation and Digital Beamforming via Linear Antenna Arrays Depending on Mutual Coupling Based on the Method of Moments," *International Journal on Communications Antenna and Propagation (IRECAP)*, vol. 14, no. 5, p. 313, Oct. 2024.

[4] A. Abuelhaija and G. Saleh, "Broadbands Four-Branch Hybrid Coupler-Based T/R Switch for 7-Tesla Magnetic Resonance Imaging," *International Journal on Communications Antenna and Propagation (IRECAP)*, vol. 12, no. 5, p. 380, Oct. 2022.

[5] M. Abuyaghi, S. Si-Mohammed, G. Shaker and C. Rosenberg, "Positioning in 5G Networks: Emerging Techniques, Use Cases, and Challenges," in *IEEE Internet of Things Journal*, vol. 12, no. 2, pp. 1408-1427, 15 Jan. 2025.

[6] S. Saeed and A. Assalem, "Beamforming for Millimeter Waves Using a Planar Fresnel Zone Plate Lens Antenna Array," *International Journal on Communications Antenna and Propagation (IRECAP)*, vol. 14, no. 6, p. 359, Dec. 2024.

[7] Y. -T. Chang, "Wideband Asymmetric Single-Pole Double-Throw Switch Based on Back-to-Back Coupler Structure," in *IEEE Solid-State Circuits Letters*, vol. 6, pp. 205-208, 2023.

[8] M. M. M. Ali, O. M. Haraz, I. Afifi, A. -R. Sebak and T. A. Denidni, "Ultra-Wideband Compact Millimeter-Wave Printed Ridge Gap Waveguide Directional Couplers for 5G Applications," in *IEEE Access*, vol. 10, pp. 90706-90714, 2022.

[9] Q. -H. Yang, L. -S. Wu, Z. -L. Xu and J. -F. Mao, "A Dual-Component Electric Probe Embedded With a 0°/180° Hybrid Coupler for Near-Field Scanning," in *IEEE Transactions on Microwave Theory and Techniques*, vol. 71, no. 3, pp. 1112-1124, March 2023.

[10] G. Diverrez, E. Kerhervé, M. D. Matos and A. Cathelin, "Compact and Slow-Wave Tunable 28 nm CMOS-SOI Twisted Hybrid Couplers for 5G Applications," in *IEEE Transactions on Microwave Theory and Techniques*, vol. 72, no. 4, pp. 2486-2497, April 2024.

[11] M. W. Almeshehe et al., "Low loss waveguide-based Butler matrix with iris coupling control method for millimeterwave applications," Waves in Random and Complex Media, vol. 33, no. 2, pp. 372–392, 2023.

[12] C. Wei, Y. Liu, J.-W. Lian, C. Geng, and D. Ding, "Millimeter-Wave Wide-Angle Ridge Gap Waveguide Multibeam Antenna Fed by 3-D Printing Butler Matrix," *IEEE Transactions on Microwave Theory and Techniques*, pp. 1–12, 2025.

[13] M. Almeshehe et al., "Surface roughness impact on the performance of the 3D metal printed waveguide coupler at millimeterwave band," Engineering Science and Technology, an International Journal, vol. 35, Nov. 2022.

[14] Y. Gao and H. C. Luong, "A 50–67-GHz Transformer-Based Six-Port Balanced-to-Unbalanced Quadrature Hybrid Coupler," in *IEEE Solid-State Circuits Letters*, vol. 7, pp. 139-142, 2024.

[15] H. Liu, T. -Y. Liu and H. Tian, "Compact 3-D Printed Phase-Shifting Coupler with Decoupling Column and Defected Ground Structures for Millimeter Wave Applications," in *IEEE Transactions on Circuits and Systems II: Express Briefs*, vol. 71, no. 4, pp. 2009-2013, April 2024.

[16] M. Y. Soliman, M. M. M. Ali, S. I. Shams, M. F. A. Sree, D. E. Fawzy, and A. M. M. A. Allam, "Ridge Gap SIW Wideband Hybrid Directional Coupler for Ka-Band Applications," in Proc. 2020 7th Int. Conf. Electrical and Electronics Engineering (ICEEE), pp. 211-214, 2020.

[17] E. Garay, M. Y. Huang, and H. Wang, "A Cascaded Self-Similar Rat-Race Hybrid Coupler Architecture and its Compact Fully Integrated Ka-band Implementation," in Proc. IEEE/MTT-S International Microwave Symposium (IMS), pp. 79-82, 2018.

[18] S. I. Shams, and A. A. Kishk, "Design of 3-dB Hybrid Coupler Based on RGW Technology," in *IEEE Transactions on Microwave Theory and Techniques*, vol. 65, no. 10, pp. 3849–3855, Oct. 2017.

[19] M. Moubadir, H. Aziz, N. A. Touhami, and A. Mohamed, "A Miniaturized Branch-Line Hybrid Coupler Microstrip for Long Term Evolution Applications," Procedia Manufacturing, vol. 22, pp. 491–497, 2018.

[20] J. G. Chi, and Y. J. Kim, "A Compact Wideband Millimeter-Wave Quadrature Hybrid Coupler Using Artificial Transmission Lines on a Glass Substrate," in *IEEE Microwave and Wireless Components Letters*, vol. 30, no. 11, pp. 1037–1040, Nov. 2020.

[21] T. Despoisse, N. Deltimple, A. Ghiotto, M. de Matos, J. Forest, and P. Busson, "An Integrated 65-nm CMOS SOI Ka-Band Asymmetrical Single-Pole Double-Throw Switch Based on Hybrid Couplers," in *IEEE Microwave and Wireless Components Letters*, vol. 30, no. 12, pp. 1157–1160, Dec. 2020.

[22] M. M. M. Ali, S. I. Shams, and A. R. Sebak, "Printed Ridge Gap SIW 3-dB Coupler: Analysis and Design Procedure," in *IEEE Access*, vol. 6, pp. 8501–8509, 2018.

[23] M. Margalef-Rovira, J. Lugo-Alvarez, A. Bautista, L. Vincent, S. Lepilliet, A. A. Saadi, F. Podevin, M. J. Barragan, E. Pistono, S. Bourdel, C. Gaquiere, and P. Ferrari, "Design of mm-Wave Slow-Wave-Coupled Coplanar Waveguides," in *IEEE Transactions on Microwave Theory and Techniques*, vol. 68, no. 12, pp. 5014–5028, Dec. 2020.

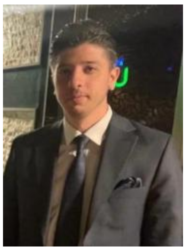

Osamah Ali Mohsin is a final - year PhD student at the University Putra Malaysia, Faculty of Engineering. Osamah's research field is Wireless Communications. Currently, Osamah is working as a lecturer at the University of Technology in Iraq, Department of Communications.

Alyani Ismail received her Bachelor of Engineering in Electronic and Information Systems Engineering from the University of Huddersfield, UK in 1999. She obtained her MSc in Computer, Communication and Human-Centred Systems from the University of Birmingham, UK (in year 2001) and PhD in Electronics Engineering also from the University of Birmingham (in year 2006). She is a professor at the Department of Computer and Communication Systems Engineering. Alyani has the expertise is in the area of Microwave Communication particularly in communication devices, materials, microwave physics, sensors as well as in defense and security technology.